Substrate Integrated Slab Waveguide and Broadband Transition from CPW

Anil Kumar Nayak, Vinit Singh Yadav, Amalendu Patnaik
Advanced Microwave Laboratory
Department of Electronics and Communication Engineering,
Indian Institute of Technology Roorkee,
Roorkee-247667, Uttarakhand, India.
Email: anayak@ieee.org; vyadav@ec.iitr.ac.in; apatnaik@ieee.org

***Abstract*—In this paper, a new broadband transition between conductor backed coplanar waveguide (CB-CPW) and substrate integrated slab waveguide (SISW) filled with a perforated dielectric medium with air vias is proposed. In order to achieve low effective permittivity and increased single-mode bandwidth without affecting the cutoff frequency of fundamental mode, the two rows of air vias are implemented in this structure. Moreover, the curved metallic row in classical substrate integrated waveguide (SIW) is used to reduce overall loss and improved impedance bandwidth of the proposed design. The proposed structure is simulated and optimized by ANSYS HFSS ver.19 and further validated experimentally.The experimental results are in agreement with the simulated results over the entire frequency band (12-18 GHz). Within the desired frequency range, the following results are obtained: return loss (RL) 15 dB, insertion loss (IL) below 0.92 dB, and overall loss variation 2-30%. This transition is suitable for Ku-band applications such as antenna, filter, amplifier, and other microwave devices.**

***Index Terms*—Broadband, CPW, Impedance bandwidth, substrate integrated slab waveguide, Substrate integrated waveguide.**

I. Introduction

Now-a-days, researchers need compact size, low loss, high power handling, and low leakage loss components for the design of antennas, microwave active, and passive circuits. The microstrip line is not fulfilling all the requirements when designed for the millimeter and terahertz wave antennas and circuits. The substrate integrated waveguide (SIW) is a new technology that provides more compact and lighter than traditional metallic waveguide but still lags of the quality factor. So far, for the mm- and THz-wave system SIW based components fulfilled the requirement of low loss, low interference, small size, full bandwidth, and the high-quality factor structures [1], [2]. It is not only better than rectangular waveguide (RW) but also have benefits than the microstrip planar based components. It leads to high quality (Q)-factor, easy fabrication and integration, more power capacity, and low losses than the microstrip line. Moreover, the SIW can be used very suitably for microwave-, mm -, and THz-wave applications. The SIW concept is first proposed in 1998 [3] and formalized in the year 2001 [4]. The initial analytical formulation of the SIW can be found in [5] and [6]. Moreover, the substrate integrated slab waveguide (SISW) techniques, was introduced in 2005 [7]. It has many advantages over SIW such as compact, moderately low losses, easy to fabricate, and cost-effectiveness. In [8], [9], It has not only provided these merits but also given more benefits like reducing effective permittivity (ϵ_{eff}), increasing the cut-off frequency of $2^{nd}-$mode, and enhancing the single-mode impedance bandwidth. Many transitions have been designed between SIW and microstrip line (MSL), co-planar waveguide (CPW), and grounded CPW [10]–[13]. In order to make low insertion loss and proper impedance matching, these have been designed and implemented. To have compact, broadband, low insertion loss, and reduced overall loss, recently, the various transitions in the forms of SIW to MSL, MSL to ridge SIW, and many more have been proposed in [14]–[16].

In this paper, a broadband transition from the conductor

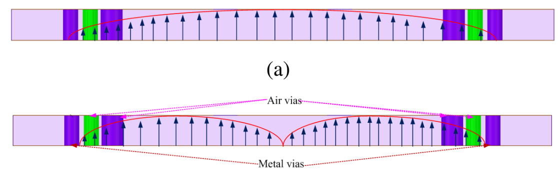

Fig. 1. Mode configuration of SISW: (a) TE_{10} (b) Quasi-TE_{20}.

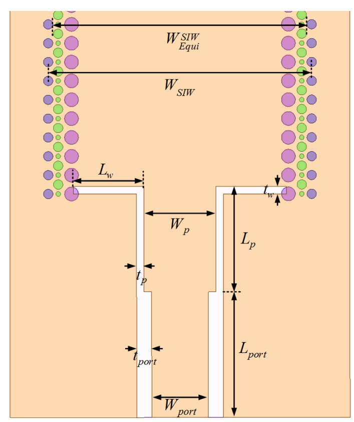

Fig. 2. The proposed CPW to SISW transition and detailed dimensions ($L_{port} = 10$, $W_{port} = 4.45$, $t_{port} = 1.2$, $W_{SIW} = 22.84$, $W_{Equi}^{SIW} = 22.42$, $L_p = 8.4$, $W_p = 5.7$, $t_p = 0.5$, $t_w = 0.46$, $L_w = 4.8$; units: millimeters).

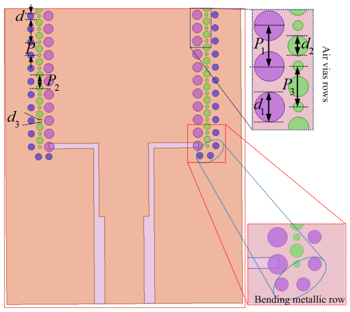

(a) (b)

Fig. 3. (a) The modified structure (b) Side view of proposed transition ($d_1 = 1.1$, $P_1 = 1.55$, $d_2 = 0.75$, $P_2 = 1.5$, $d_3 = 0.375$, $P_3 = 1.5$, $d = 0.75$, $P = 1.5$, $h = 1.524$; unit: millimeters).

backed-coplanar waveguide (CB-CPW) to substrate integrated slab waveguide (SISW) is designed, analyzed, and experimentally validated. The design was initiated from a CB-CPW to SIW transition along with a single quarter-wave ($\lambda_g/4$) transformer at the feeding network. Then, two rows of air vias are added in front of metallic vias, located precisely parallel with the metallic row. These air vias provides the low effective permitivity (ϵ_{eff}) and enhanced singe mode (SM) impedance bandwidth. Besides this, the curved metallic row is implemented for increasing of the bandwidth. The proposed transition is designed, simulated, and verified experimentally of the Ku-band frequency range. This design reduces the insertion loss, improves the return loss, and provides broadband impedance bandwidth.

II. Transition Structure

The substrate integrated slab waveguide (SISW) structure, air holes are implemented to achieve enhanced SM-impedance bandwidth. However, it is not practically affected by side portion by the fundamental mode (TE_{10}) when removing the dielectric material from vias, as shown in Fig. 1. The maximum electric field ($\vec{E}$) can be found in the middle section and vanishes in the sides. On the other hand, the second-mode has the maximum $\vec{E}$ in the side section of the design, which is called quasi $TE_{20}-$mode as shown in Fig. 1 (b). Due to air vias presence, the cutoff frequency of f_c and SM increases with a decrease in ϵ_{eff}. As a result, air vias are allowed to surge the SM-impedance bandwidth without affecting the fundamental mode.

The transition between the conductor backed-coplanar waveguide (CB-CPW) to SIW and a stepped quarter-wave ($\lambda_g/4$) transformer in the feeding part of the structure is designed, as shown in Fig. 2. At first, f_c=9.6 GHz of the desired frequency band has been chosen. Thereafter, the frequency range impedance bandwidth is calculated in $1.25f_c - 1.9f_c$ range [14], which is 12-18.24 GHz. The next step of the design structure has been matched to impedance of 50 Ohms to the fed section, whereas the length $\lambda_g/4$ transformer is kept approximately equal to $\lambda_g/4$. However, the width of $\lambda_g/4$ transformer is fixed by using of parametric analysis. The dimensions of diameter d, pitch P, W_{SIW}, and W_{Equi}^{SIW} were calculated, which has been given in [14]. The proposed transition and their dimensions are mentioned in Fig. 2 and 3. Due to more losses found by using design in the Fig. 2, the modified design is proposed, as shown in Fig. 3 (a). The previous structure's difference to the proposed design is the only curve shape metallic row at each corner of the feeding end. The beauty of these curve shape metallic rows lies in providing the reduced lateral leakages, which helps to enhance the impedance bandwidth and reduce the overall losses. The side view of the proposed structure is shown in Fig. 3 (b).

The parametric analysis effect on width t_w and length L_w of the proposed structure analyzed, as shown in Fig. 4 (a) and (b). In Fig. 4 (a), the return loss (RL) and insertion loss (IL) effect on width t_w in the proposed transition. The RL is significantly surged as clearly shown in the plot. Whereas the maximum IL is found 1.88 dB in the whole pass band ($1.25f_c - 1.9f_c$). Conversely, the IL is also found maximum 4.84 dB at 14.59 GHz. At the end, the t_w is fixed at 0.46 mm. Similarly, the variation of L_w has affected on the impedance matching and losses. Consequently, We have done parametric analysis and fixed the dimension of L_w at 4.8 mm, which is depicted in Fig. 4 (b). This transition propagates both TE_{10} and TE_{20} modes. The field configuration of electric (E) and magnetic (H) fields are shown in Fig. 5 (a) and (b), respectively. Moreover, The

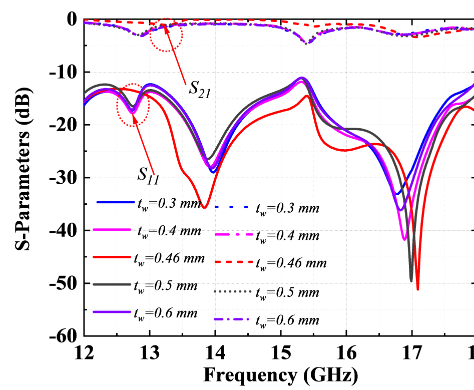

(a)

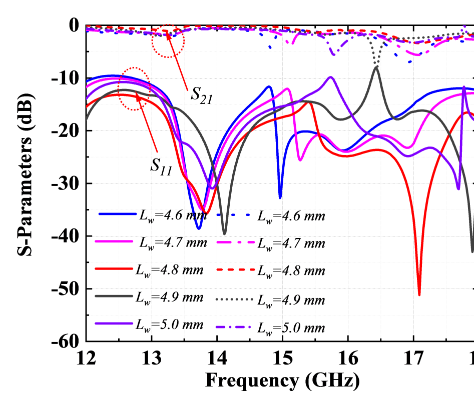

(b)

Fig. 4. S-parameters effect of (a) t_w and (b) L_w.

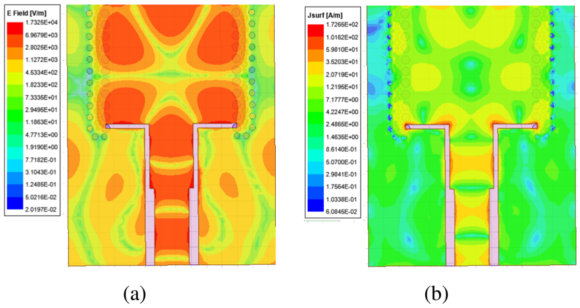

Fig. 5. (a) Electric field and (b) Surface current distribution of proposed to transition at 17.1 GHz.

maximum E-field is getting at starting of SIW and feed section. Similarly, the H-field obtained as same phase at beginning of SIW. In order to reduce the overall loss and perfect impedance matching, the metallic curved rows are implemented in the final design. The curve plays a significant primary role to stop the lateral leakage and provide the wider bandwidth. The S-parameters response of proposed final structure is compared with the previous design, as shown in Fig. 6 (a). From this plot, we can observe that both RL and IL are found better in the case of the final proposed transition. The structure is designed on a single layer substrate, Roger RT/duroid 5880 (TM) having a dielectric constant (ε_r) of 2.2, thickness (h) of 1.524 mm and loss tangent ($tan\delta$) of 0.0009. All the simulation carried out by using electromagnetic software ANSYS HFSS ver. 19.

III. Experimental Validation

The laboratory prototype of the top and bottom view of the proposed transition are shown in Fig. 6 (b). The simulated and experimented results of S parameters (S_{11} and S_{21}) of the proposed transition is shown in Fig. 6 (b). The measured results shows that the RL is above 15 dB (simulated: > 15 dB) obtained and IL is below 0.92 dB (simulated:0.37 dB) achieved in entire frequency bands (i.e. $1.25f_c - 1.9f_c$). It can be noticed that from the plot, the simulated RL is found to be above 13 dB in 12-13.25 GHz (measured:12.47 dB in 17.25-17.75 GHz) frequency range. The simulated IL is found below 2.46 dB in 16.82-17.6 GHz (measured: 2.56 dB in 16.65-17.7 GHz) frequency range. From Fig. 6 (c), the phase of S_{21} is a significant parameter of the transition, because most of the power is lost due to the time of filling of copper paste into vias in SIW. The measured and simulated results of the phase of S_{21} are shown in Fig. 6 (c). The measured and simulated results of total loss of the proposed transition are shown in Fig. 6 (d). Although the measured total loss of the proposed transition is almost the same as the simulated one, but has slightly increased by $10-20\%$. Finally, it has observed that the measured result is found in good agreement with the simulated one.

IV. Conclusion

This paper presents a new type of broadband transition between CB-CPW and SISW by using a metallic curved row. The proposed transition has acceptable good return loss,

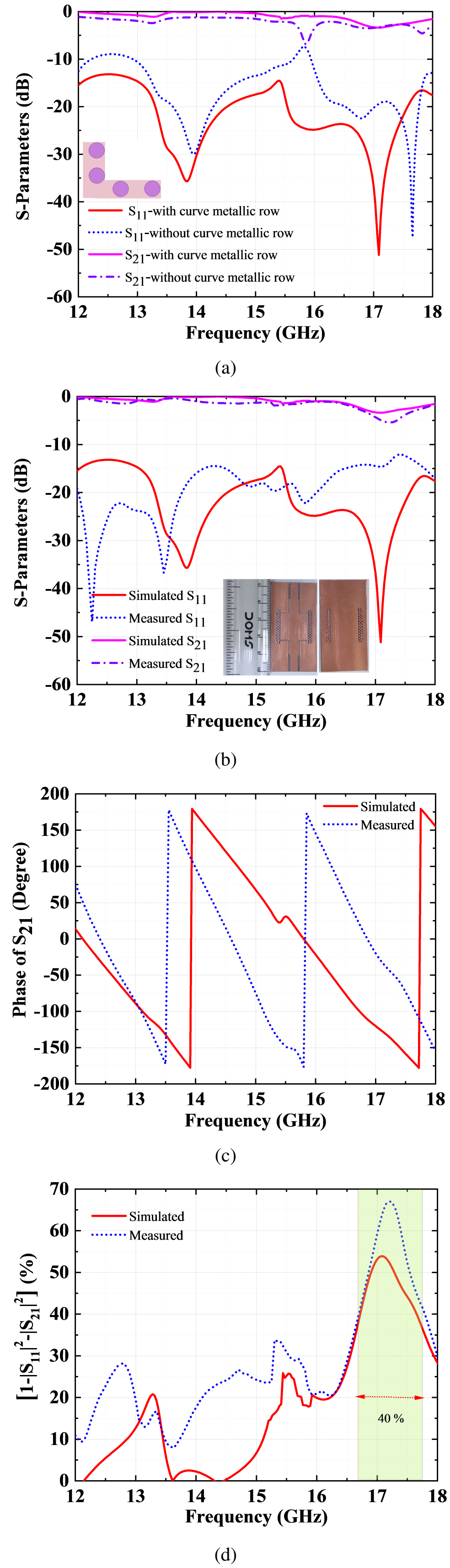

Fig. 6. Characteristics of the transition: (a) $|S_{11}|$ and $|S_{21}|$ with and without curved metallic row (b) $|S_{11}|$ and $|S_{21}|$, (c) Phase of S_{21}, and (d) Total loss.

low insertion loss, wider bandwidth, and better impedance matching in the whole passband. This transition is suitable for different microwave applications in the Ku-band frequency range.

REFERENCES

[1] D. Deslandes, "Design equations for tapered microstrip-to-substrate integrated waveguide transitions," in *2010 IEEE MTT-S International Microwave Symposium*, 2010, pp. 704–707.

[2] Z. Kordiboroujeni and J. Bornemann, "New wideband transition from microstrip line to substrate integrated waveguide," *IEEE Transactions on Microwave Theory and Techniques*, vol. 62, no. 12, pp. 2983–2989, 2014.

[3] A. Tugulea and I. R. Ciric, "Two-dimensional equations for microwave planar circuits," in *1998 Symposium on Antenna Technology and Applied Electromagnetics*, Aug 1998, pp. 315–318.

[4] D. Deslandes and K. Wu, "Integrated microstrip and rectangular waveguide in planar form," *IEEE Microwave and Wireless Components Letters*, vol. 11, no. 2, pp. 68–70, 2001.

[5] Y. Cassivi, L. Perregrini, P. Arcioni, M. Bressan, K. Wu, and G. Conciauro, "Dispersion characteristics of substrate integrated rectangular waveguide," *IEEE Microwave and Wireless Components Letters*, vol. 12, no. 9, pp. 333–335, Sep. 2002.

[6] D. Deslandes and Ke Wu, "Single-substrate integration technique of planar circuits and waveguide filters," *IEEE Transactions on Microwave Theory and Techniques*, vol. 51, no. 2, pp. 593–596, Feb 2003.

[7] M. Bozzi, D. Deslandes, P. Arcioni, L. Perregrini, K. Wu, and G. Conciauro, "Efficient analysis and experimental verification of substrate-integrated slab waveguides for wideband microwave applications," *International Journal of RF and Microwave Computer-Aided Engineering*, vol. 15, no. 3, pp. 296–306, 2005.

[8] M. Bozzi, D. Deslandes, P. Arcioni, L. Perregrini, K. Wu, and G. Conciauro, "Analysis of substrate integrated slab waveguides (sisw) by the bi-rme method," in *IEEE MTT-S International Microwave Symposium Digest, 2003*, vol. 3, 2003, pp. 1975–1978 vol.3.

[9] E. Massoni, L. Silvestri, G. Alaimo, S. Marconi, M. Bozzi, L. Perregrini, and F. Auricchio, "3-d printed substrate integrated slab waveguide for single-mode bandwidth enhancement," *IEEE Microwave and Wireless Components Letters*, vol. 27, no. 6, pp. 536–538, 2017.

[10] D. Deslandes and K. Wu, "Integrated microstrip and rectangular waveguide in planar form," *IEEE Microwave and Wireless Components Letters*, vol. 11, no. 2, pp. 68–70, 2001.

[11] A. Suntives and R. Abhari, "Transition structures for 3-d integration of substrate integrated waveguide interconnects," *IEEE Microwave and Wireless Components Letters*, vol. 17, no. 10, pp. 697–699, 2007.

[12] T. Zhang, L. Li, Z. Zhu, and T. J. Cui, "A broadband planar balun using aperture-coupled microstrip-to-siw transition," *IEEE Microwave and Wireless Components Letters*, vol. 29, no. 8, pp. 532–534, 2019.

[13] F. Taringou, T. Weiland, and J. Bornemann, "Broadband design of substrate integrated waveguide to stripline interconnect," in *2014 International Conference on Numerical Electromagnetic Modeling and Optimization for RF, Microwave, and Terahertz Applications (NEMO)*, 2014, pp. 1–4.

[14] A. K. Nayak, V. Singh Yadav, and A. Patnaik, "Wideband transition from tapered microstrip to corrugated siw," in *2019 IEEE MTT-S International Microwave and RF Conference (IMARC)*, 2019, pp. 1–4.

[15] D. Herraiz, H. Esteban, J. A. MartÃnez, A. Belenguer, and V. Boria, "Microstrip to ridge empty substrate-integrated waveguide transition for broadband microwave applications," *IEEE Microwave and Wireless Components Letters*, vol. 30, no. 3, pp. 257–260, 2020.

[16] A. Belenguer, J. A. Ballesteros, M. D. Fernandez, H. E. GonzÃ¡lez, and V. E. Boria, "Versatile, error-tolerant, and easy to manufacture through-wire microstrip-to-esiw transition," *IEEE Transactions on Microwave Theory and Techniques*, vol. 68, no. 6, pp. 2243–2250, 2020.